

## Initiation and propagation of laminar spherical flames at atmospheric pressure<sup>†</sup>

Nikolai M. Rubtsov,<sup>\*a</sup> Boris S. Seplyarskii,<sup>a</sup> Kirill Ya. Troshin,<sup>b</sup>  
 Victor I. Chernysh<sup>a</sup> and Georgii I. Tsvetkov<sup>a</sup>

<sup>a</sup> Institute of Structural Macrokinetics and Materials Science, Russian Academy of Sciences, 142432 Chernogolovka, Moscow Region, Russian Federation. Fax: +7 495 962 8025; e-mail: nmrubtss@mtu-net.ru

<sup>b</sup> N. N. Semenov Institute of Chemical Physics, Russian Academy of Sciences, 119991 Moscow, Russian Federation

DOI: 10.1016/j.mencom.2011.07.016

The influence of CO<sub>2</sub>, Ar, propylene and CCl<sub>4</sub> additives on the initial stages and dynamics of flame front formation and the structure of laminar spherical flames in hydrogen–air, methane–air and *n*-pentane–air mixtures at atmospheric pressure has been demonstrated by means of colour high-speed digital cinematography.

The dynamics of formation of a stationary flame front (FF) of a combustible mixture at spark ignition remains a scantily known area of combustion physics.<sup>1–5</sup> Earlier,<sup>5</sup> the propagation of laminar spherical flames in stoichiometric mixtures of natural gas and isobutylene with oxygen in the presence of Kr and CO<sub>2</sub> in a bomb of a constant volume at total pressures up to 100 Torr was studied by means of colour high-speed digital cinematography. It was shown that, on dilution of gas mixtures with Kr and CO<sub>2</sub>, the time of steady FF formation increases by a factor of >10; the influence of CO<sub>2</sub> on hydrocarbon combustion is stronger than that of Kr; the relation of times of FF formation is in inverse proportion to the corresponding relation of warming-up in these flames.

The aim of this work was to study the dynamics of gaseous steady FF formation and propagation at atmospheric pressure by means of high-speed colour cinematography.

The experiments were performed with stoichiometric methane–air and *n*-pentane–air mixtures diluted with inert additives (CO<sub>2</sub> and Ar) at 1 atm and 298 K. Influence of chemically active additives on hydrocarbon combustion was investigated by the addition of 2% CCl<sub>4</sub> to a stoichiometric mixture of 90% (*n*-pentane–air) + 10% CO<sub>2</sub>. The mixtures of 40% H<sub>2</sub> + 60% air with 1–2% propylene additive; 12.5% H<sub>2</sub> + 87.5% air and 10% H<sub>2</sub> + 90% air without additives were also used in experiments. 1–2% CCl<sub>4</sub> were added to these mixtures for FF visualization.<sup>‡</sup> Note that these amounts of CCl<sub>4</sub> do not influence the regularities of hydrogen–air combustion.<sup>3</sup>

The pressure during combustion was recorded by pressure transducers. The time dependence of the sphere radius  $R(t)$  filled with products of combustion was calculated from initial sites of pressure growth curves<sup>1</sup> obtained in the course of combustion:

$$\frac{R(t)}{R_0} = \left\{ 1 - \frac{[P_b - P(t)][P(t)/P_0]^{-1/\gamma}}{P_b - P_0} \right\}^{1/3} \quad (1)$$

<sup>†</sup> The electronic version of this article includes video clips for Figures 1(b),(c), 3(a),(b) and 4(c),(d).

<sup>‡</sup> Experiments were performed in a stainless steel reactors 14 cm in length and 13 cm in diameter (reactor 1) and 25 cm in length and 12 cm in diameter (reactor 2) supplied with optical quartz windows 12 cm in diameter on the butt-ends. Spark ignition electrodes were placed in the centres of the reactors. The pumped reactors were filled with test gas mixtures to 1 atm; initiation was provided by a spark discharge (1.5 J, reactor 1 and 0.92 J, reactor 2). Note that the combustible mixture could be kept in the reactor for several days before initiation; *i.e.*, heterogeneous reactions were slow. Combustion was recorded by means of a Casio Exilim F1 Pro colour high-speed digital camera (60–1200 frames per second), sensitive over the spectral range of 420–740 nm. Before each experiment, the reactors were pumped out to 10<sup>–2</sup> Torr.

Here,  $R_0$  is the reactor radius,  $P_b$  is the maximal pressure,  $P_0$  is the initial pressure,  $P(t)$  is the current pressure of a gas mixture, and  $\gamma = 1.2$  is the ratio of specific heats.<sup>1</sup> From the time dependence of  $R(t)$ , normal flame velocity  $Un = [dR(t)/dt]/\varepsilon_T$  was calculated. The value of  $\varepsilon_T$  was determined from the maximal pressure of combustion  $P_b$ :<sup>1</sup>

$$P_b/P_0 = 1 + \gamma(\varepsilon_T - 1). \quad (2)$$

Equations (1) and (2) were used for calculation of flame velocities, which were also independently determined from the change of the visible radius of a spherical flame.

Typical results of filming the process of FF formation and propagation for diluted stoichiometric *n*-pentane–air mixtures are shown in Figure 1. A delay period in the development of initiation centres is observed in the combustion of a diluted mixture (*n*-pentane–air)<sub>stoich</sub> + 10% CO<sub>2</sub> [frames 2–11, Figure 1(a)] in reactor 1, as it was observed<sup>5</sup> for diluted mixtures at lower pressures.

Dynamics of increase in the visible radius of spherical FF for various combustible mixtures was determined from the sequences of images in reactor 2 (Figure 2). These results were independently obtained both by means of image processing of video clips of combustion process [Figure 2(a)] and from the initial sites of pressure growth curves obtained in the course of combustion using equations (1) and (2) [Figure 2(b)]. From Figure 2, it is possible to determine the time of steady FF formation  $\tau_f$ . In Figure 2(a),  $\tau_f$  is the moment of the origination of linear time dependence of FF coordinate and in Figure 2(b) it is the point of intersection of time dependence of FF coordinate with the  $x$ -coordinate. As is seen in Figure 2, the results of measurement of FF velocities with both methods (*e.g.*, the experimental value of  $Un$  in stoichiometric methane–air mixture is 30±2 cm s<sup>–1</sup>) are in good agreement with published data<sup>5</sup> (5–35 cm s<sup>–1</sup>). Both methods independently show that, in diluted mixtures, a constant flame velocity is reached in the certain time interval corresponding to the time  $\tau_f$  of steady FF formation.

Figure 2 demonstrates that the closer the combustible mixture to a limit of initiated ignition, the longer  $\tau_f$ . The processing of experimental data on the change of visible radius of a spherical flame for diluted mixtures allowed one to determine the lower range value of the radius of the initial centre of combustion from which the stationary combustion<sup>6–8</sup> develops. This radius is 0.3 cm for both CO<sub>2</sub> and Ar [Figure 2(a)]; CO<sub>2</sub> additives are more effective than those of Ar.<sup>5</sup>

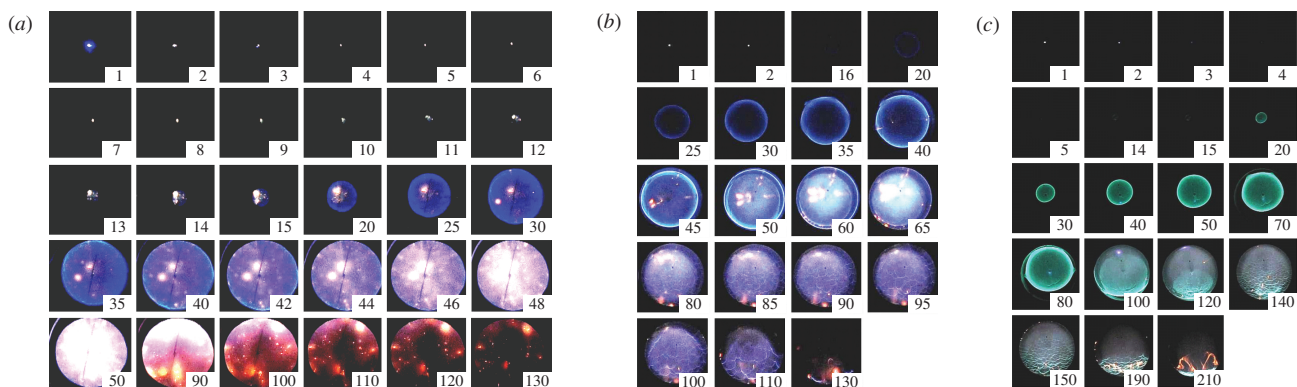


**Figure 1** Sequences of video images (with consecutive numbers) of the propagation of spherical FF. 600 frames per second. (*n*-pentane + air)<sub>stoich</sub> + 10% CO<sub>2</sub>,  $T_0 = 298$  K. (a)  $E_0 = 1.51$  J, reactor 1; (b)  $E_0 = 0.91$  J, reactor 2; (c) + 2% CCl<sub>4</sub>,  $E_0 = 0.91$  J, reactor 2. To start playback of the video clips in the electronic version of the article, click on any image of Figures 1(b),(c).

We observed that cellular structures occur on FF after a contact of FF with lateral walls of reactor 2 [for example, frame 110 in Figure 1(b)]; the average cell size decreases with the concentration of an inert diluent (CO<sub>2</sub> or Ar). At flame propagation to butt-ends of the cylindrical reactor, cellular structures move in a gravity direction [Figure 1(b),(c)]; in this case, combustion products fill the upper part of the reactor and cold unburnt mixture in the bottom of reactor butt-end burns in cellular regime. In addition, Figure 1(a) shows that cellular structures are missing in the reactor 1, in which spherical FF almost simultaneously touches top, bottom and lateral reactor walls. The latter fact substantiates our conclusion that cellular regimes due to the hydrodynamic instability of FF under gravity should probably occur in reactors, in which FF can propagate horizontally into cold unreacted gas to produce convective flows.

Cellular flames can occur<sup>1</sup> in nonstoichiometric flames; the marked difference in diffusivity, for example, of a missing reagent, and thermal diffusivity of combustible mixture (thermo-diffusive instability) is a necessary condition for cellular structure formation. According to a mechanism,<sup>1</sup> cellular flame should not occur in stoichiometric mixtures.

The aforesaid is illustrated in Figure 3, where the result of filming of FF propagation in a lean mixture of 12.5% H<sub>2</sub> + 87.5% air illuminated by 2% CCl<sub>4</sub> is shown. FF has, as a whole, a spherical form with the perturbations whose amplitude increases with flame radius; the flame radius can be estimated from Figure 3(a). The normal flame velocity  $Un = Vv/\varepsilon_T$  ( $Vv$  is the visible flame velocity) determined from Figure 3(a) using equations (2) and (3) is 50 cm s<sup>-1</sup>. The normal flame velocity for the mixture of 10% H<sub>2</sub> + 90% air is 21 cm s<sup>-1</sup>. These values correlate well with literature data,<sup>9</sup> and they are close to the results of numerical calculations of  $Un$  obtained by means of a laminar flame model.<sup>10,11</sup> It means that perturbations observed on FF do not render essential influence on its velocity at least for H<sub>2</sub> > 10% in air.

In the immediate vicinity of ignition limit of diluted (with CO<sub>2</sub> or Ar) mixtures, repeated initiation by a spark discharge (with an interval ~1–2 s between discharges) is required for the initiation of flame propagation. It is possible evidence of the important role of low-temperature reactions at an ignition limit, namely, a certain part of spark discharge energy is spent for the formation of long-lived active intermediates (hydroperoxides, aldehydes, etc.<sup>3</sup>). The occurrence of these particles facilitates ignition as

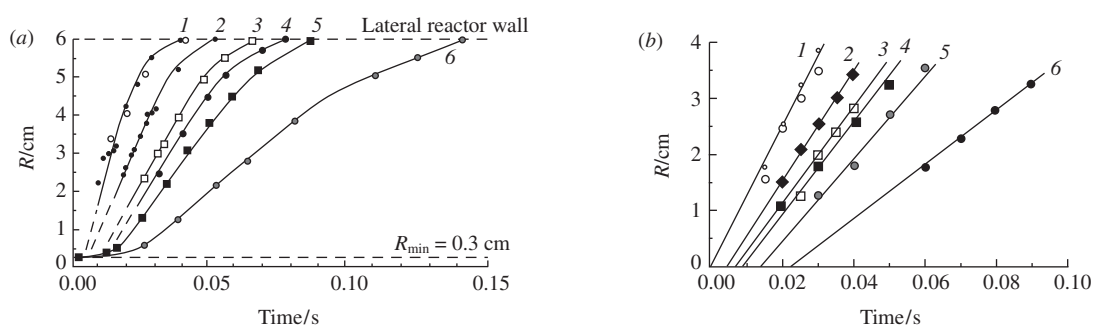


**Figure 2** The time dependence of the increase in visible radius  $R$  of emission of spherical FF on the composition of the mixture (298 K), reactor 2. (1) 90% (methane + air)<sub>stoich</sub> + 10% Ar, (2) 95% (methane + air)<sub>stoich</sub> + 5% CO<sub>2</sub>, (3) 80% (*n*-pentane + air)<sub>stoich</sub> + 20% Ar, (4) 90% (*n*-pentane + air)<sub>stoich</sub> + 10% CO<sub>2</sub>, (5) 89.5% (*n*-pentane + air)<sub>stoich</sub> + 10% CO<sub>2</sub> + 0.5% CCl<sub>4</sub>, (6) 88% (*n*-pentane + air)<sub>stoich</sub> + 10% CO<sub>2</sub> + 2% CCl<sub>4</sub>. (a) Calculated from an increase in the visible front radius of a laminar flame; (b) calculated from the initial sites of pressure growth curves.

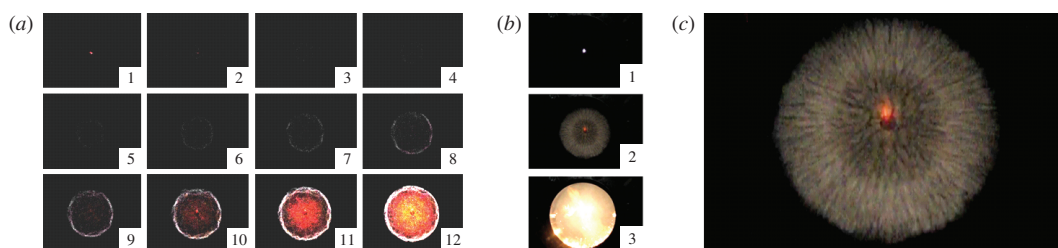


**Figure 3** Sequences of video images (with consecutive numbers) of propagation of spherical FF illuminated by 2% CCl<sub>4</sub>, in mixture 12.5% H<sub>2</sub> + 87.5% air, reactor 2. (a) 300 frames per second; (b) 60 frames per second; (c) enlarged frame 2 of Figure 3(b). To start playback of the video clips in the electronic version of the article, click on any image of Figures 3(a),(b).

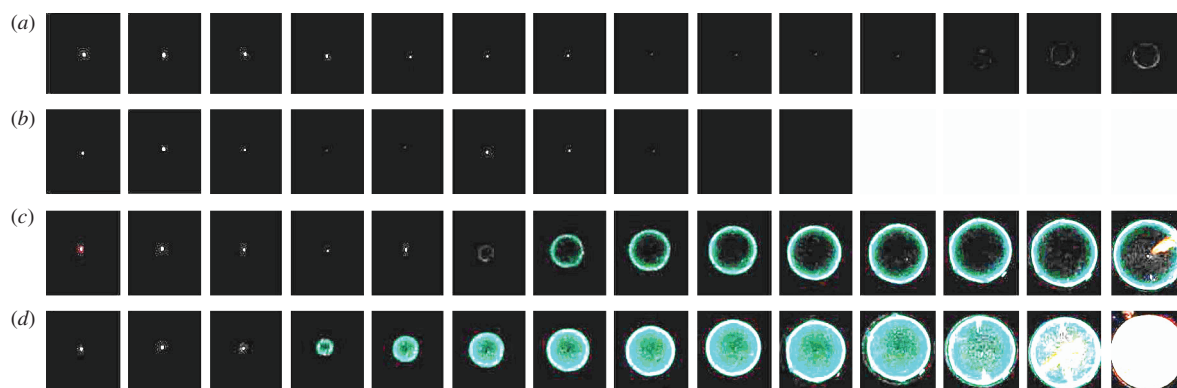


**Figure 4** Sequences of video images of propagation of spherical FF in mixture 40%  $\text{H}_2$  + 60% air in the presence of propylene. The front of a hydrogen flame is illuminated by the additive of 2%  $\text{CCl}_4$ , reactor 2. 1200 frames per second. (a) 2% of propylene, the 6<sup>th</sup> consecutive initiation by the spark discharge; (b) 2% of propylene, the 3<sup>rd</sup> consecutive initiation by the spark discharge; (c) 1.5% of propylene, the 1<sup>st</sup> initiation by the spark discharge; (d) 1% of propylene, the 1<sup>st</sup> initiation by the spark discharge. To start playback of the video clips in the electronic version of the article, click on any image of Figures 4(c),(d).

they quickly break up or react with formation of chain carriers (free atoms and radicals)<sup>3,4</sup> at higher temperatures in a discharge zone. Such repeated spark initiation provides an increase in temperature in the vicinity of a spark discharge area that also should facilitate ignition.

To understand the nature of an initial stage of ignition in a combustible gas mixture, it is reasonable to use the results obtained for a problem of hot spot thermal explosion. The problem of critical conditions of hot spot thermal explosion, as well as the analysis of non-stationary ignition of a hot spot for a zero order chemical reaction, was considered in refs. 7 and 8. The problem of hot-spot ignition can be reduced to the examination of dynamics of a reaction zone on cooling of the hot spot with inert environment. Eventually the cooling of substance at the surface of the hot spot occurs and the border of a reaction zone moves to the centre of the hot spot. If by the time when an adiabatic induction period has not yet elapsed the size of a reaction zone becomes such that the heat cannot be removed, the hot spot ignites. Thus, for hot spot ignition, it is necessary that, during an adiabatic induction period, the size of a reaction zone does not become less than a critical size. The sequences of frames shown, for example, in Figures 1(a),(c), allow one to consider that this model qualitatively describes hot spot evolution. However, the described model does not take into account the chemical mechanism of process, which can reveal itself in strong influence of small chemically active additives on the critical size of a hot spot. This is demonstrated in Figure 1(b),(c). The  $\text{CCl}_4$  additive provides a marked increase in  $\tau_f$  and respective reduction of flame velocity.

A considerable influence of a small chemical additive (propylene) on  $\tau_f$  was also observed for hydrogen combustion. In Figure 4(a),(d) the result of high-speed filming of steady FF formation in the mixture 40%  $\text{H}_2$  + 60% air, illuminated with 2%  $\text{CCl}_4$  in the presence of 1, 1.5 and 2% propylene is shown. We noticed that, in the same mixture but without  $\text{C}_3\text{H}_6$ , FF reached an upper edge of an optical window by the third frame after spark initiation. It means that the small  $\text{C}_3\text{H}_6$  additive (1–2%) provides a marked reduction of flame velocity. Note that the propagation of an  $\text{H}_2$ –air flame in the presence of 2% propylene is observed only after six consecutive spark initiations of the mixture [Figure 4(d)]. Figure 4(c) corresponds to the third initiation by spark discharge; the initial centre of combustion was formed, but it did not provide flame propagation.

The data shown in Figures 1 and 4 specify that the real evolution pattern of a combustion centre of hydrogen and hydrocarbon oxidation in the presence of a chemically active additive cannot be well described with the model in which the chemistry of the process is represented by only one reaction in the form of Arrhenius

law. This is testified by both strong influence of chemically active additive on the period of steady FF formation and the occurrence of critical conditions of initiation. Hence, in the theoretical analysis of a problem of hot spot ignition in gaseous combustion, it is necessary to consider not only cooling the hot spot with an inert environment but also the fluxes of active centres (atoms and radicals) into unreacted gas.

Thus, we were the first to observe cellular flames in diluted stoichiometric hydrocarbon–air mixtures after contact of a flame front with reactor walls. Colour high-speed cinematography allowed us to establish that, at spark ignition in the vicinity of initiation limit of a gas mixture, the initial combustion centre of a minimum size, from which the stationary combustion wave develops, is formed.

We are grateful to Professor A. A. Borisov (N. N. Semenov Institute of Chemical Physics, Russian Academy of Sciences) for valuable remarks.

This work was supported in part by the Russian Foundation for Basic Research (projects nos. 09-03-00622-a and 10-08-00305-a).

## References

- Ya. B. Zel'dovich, G. I. Barenblatt, V. B. Librovich and G. M. Machviladze, *Matematicheskaya teoriya goreniya i vzryva (Mathematical Theory of Combustion and Explosion)*, Nauka, Moscow, 1980 (in Russian).
- G. I. Ksandopulo and V. V. Dubinin, *Khimiya gazofaznogo goreniya (Chemistry of Gaseous Combustion)*, Khimiya, Moscow, 1987 (in Russian).
- B. Lewis and G. Von Elbe, *Combustion, Explosions and Flame in Gases*, Academic Press, New York, London, 1987.
- J. Warnatz, U. Maas and R. W. Dibble, *Combustion: Physical and Chemical Fundamentals, Modeling and Simulation, Experiments, Pollutant Formation*, 3<sup>rd</sup> edn., Springer-Verlag, Berlin, 2001.
- V. I. Chernysh, N. M. Rubtsov, B. S. Septyarskii and G. I. Tsvetkov, *Mendeleev Commun.*, 2009, **19**, 230.
- A. I. Rozlovskii, *Osnovy tekhniki vzryvobezopasnosti pri rabote s goryuchimi gazami i parami (Fundamentals of Fire Protection when Operating with Combustible Gases and Vapors)*, Khimiya, Moscow, 1987 (in Russian).
- B. S. Septyarskii and S. Yu. Afanas'ev, *Khim. Fiz.*, 1989, **8**, 646 [*Chem. Phys. Rep. (Engl. Transl.)*, 1989, **17**, 669].
- B. S. Septyarskii and S. Yu. Afanas'ev, *Fiz. Goreniya Vzryva*, 1989, **22**, 9 (in Russian).
- D. Liu and R. MacFarlane, *Combust. Flame*, 1983, **49**, 59.
- N. M. Rubtsov, B. S. Septyarskii, V. I. Chernysh and G. I. Tsvetkov, *Mendeleev Commun.*, 2008, **18**, 220.
- P. Saxena and F. A. Williams, *Combust. Flame*, 2006, **145**, 316.

Received: 20th January 2011; Com. 11/3665